Hybrid-PIC Simulation of Hall Thruster with Internally Mounted Cathode

IEPC-2017-429

Presented at the 35th International Electric Propulsion Conference
Georgia Institute of Technology • Atlanta, Georgia • USA
October 8 – 12, 2017

Kenichi Kubota[1]
Japan Aerospace Exploration Agency, Chofu, Tokyo, 182-8522, Japan

Shinatora Cho[2]
Japan Aerospace Exploration Agency, Sagamihara, Kanagawa, 252-5210, Japan

Hiroki Watanabe[3]
Tokyo Metropolitan University, Hino, Tokyo, 191-0065, Japan

and

Ikkoh Funaki[4]
Japan Aerospace Exploration Agency, Sagamihara, Kanagawa, 252-5210, Japan

Abstract: The plasma flow of SPT-100 with an imaginary internal cathode was simulated by using hybrid-PIC model. In the model, anomalous resistivity along the magnetic field is considered to reduce excessive electron transport along the magnetic field, and to realize stable numerical procedures in a regular mesh. The results show that the basic properties such as isothermal characteristics of electron temperature along the magnetic field can be well captured in a regular mesh in spite of the newly added resistivity along the magnetic field. It is also shown that potential well in front of the internal cathode can be formed by reducing the extent of Bohm diffusion around the cathode.

Nomenclature

a	=	coefficient of anomalous resistivity model
b	=	coefficient of anomalous resistivity model
B	=	magnetic flux density
e	=	elementary charge
E	=	electric field
j	=	current density
k	=	Boltzmann constant
n	=	number density
m	=	mass of particle
q	=	thermal flux
T	=	temperature
u	=	velocity

[1] Researcher, Aeronautical Technology Directorate, kubota.kenichi@jaxa.jp
[2] Researcher, Research and Development Directorate, choh.shinatora@jaxa.jp.
[3] Research Associate, Department of Aerospace Engineering, hwatanabe@tmu.ac.jp.
[4] Associate Professor, Institute of Space and Astronautical Science, funaki@isas.jaxa.jp.

α_B	=	coefficient of Bohm diffusion
β	=	Hall parameter
μ	=	mobility
ν	=	collision frequency
ρ	=	mass density
ϕ	=	electric potential
ω	=	angular frequency
subscript		
c	=	cyclotron
e	=	electron
i	=	ion
n	=	neutral
sh	=	sheath
w	=	wall

I. Introduction

FOR the main propulsion system of all-electric satellite which is believed to realize significant improvement of a payload capability, R&Ds of high power Hall thrusters (>5kW) are energetically being carried out in many universities, research organizations and companies.[1-3] In Japan, capabilities of both TAL and SPT type Hall thrusters in that power range are explored to expand the range of options in the future. JAXA, IA, IHI, and Tokyo Metropolitan University (TMU) are focused on the R&D of SPT type Hall thruster in the 2-6 kW power range where broad utility is expected.[4]

In understanding all effects determining the thrust efficiency, the cathode coupling and position is one of the most important concerns. Since the high power Hall thrusters has relatively larger diameter, proper design of the thruster head allows the internally mounted cathode which is known to have higher thrust efficiency by several percent than the externally mounted cathode condition due to better cathode coupling.[5] Such a totally axisymmetric configuration enables us to simulate the near-field plasma by using two-dimensional axisymmetric model. JPL has been developing H6 and HERMeS thrusters which employ internally mounted cathodes, and also developing Hall2De code which employs fluid model for the all species.[6] The code can simulate the plume plasma of the thrusters from the center-positioned cathode boundary. Hybrid-PIC (Particle In Cell) simulation of the plume region is also going on in Michigan University.[7]

The Hall thruster being developed in JAXA has also an internally mounted cathode, and experimental and numerical evaluation of the thrust performance have been conducted. As the numerical efforts, we are developing numerical simulation tools called JHAST f/p (full-PIC)[8] and h/p (hybrid-PIC). This study focuses on the numerical evaluation of the plasma flow regarding the Hall thruster with the internally mounted cathode by using JHAST h/p in which the heavy particles (neutrals and ions) and electrons are modeled as particles and fluid, respectively. JHAST h/p was originally developed for the simulation of hollow cathodes,[9,10] and was expanded to enable the simulation of the acceleration channel as well.[11] The model we employed does not require the mesh aligned mesh, which has been used in the hybrid-model for Hall thrusters,[12-15] owing to the use of additional resistivity along the magnetic field. With this model, this paper focuses on the not only the acceleration channel but also the plume from the internal cathode. Through the comparison with the preceding studies on the flow field, the validation of the developing code is discussed.

II. Numerical Modeling

A. Thruster

In this paper, SPT-100 was selected as a thruster geometry because of its abundant references, whereas the actual SPT-100 does not have an internal cathode. Qualitative discussion on the internal cathode, however, is possible even with this imaginary thruster, and we expect that the performance and flow fields will not be affected drastically even if an imaginary internal cathode is virtually installed at the center of the thruster. The configuration and the magnetic flux density distribution is shown in Fig. 1. It was assumed that an internal cathode which has a keeper-orifice diameter of 5 mm is set, from which cathode plasma is come out uniformly. The keeper wall is not distinguished as a conductor for simplicity, i.e. it is treated as a dielectric material (Boron nitride) as the channel walls and the pole covers. The anode is set at z = 0 mm, and has propellant port of 5 mm in diameter at its center. The computational domain is extended up to 125 mm (z = 0 at anode) in the downstream direction to capture the electron's stream in the plume region.

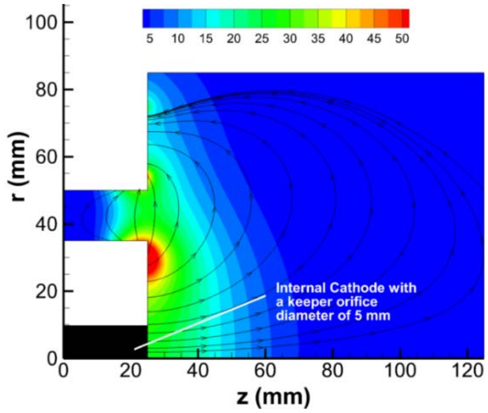

Figure 1. Thruster Geometry and Magnetic Flux Density, mT.

B. Hybrid-PIC Model

In the physical model used here, the electrons and ions are modeled as fluid and particles, respectively. The quasi-neutrality was assumed, i.e. the electron density is equal to the ion density obtained from ion PIC. Then the thin sheath assumption should be imposed on the wall boundaries. Not only the ions but also the neutrals were also modeled as particles, and the elastic collisions (n-n, n-i, i-i) and the charge exchange collision (CEX) were taken into account. The ionization by electron impact on neutrals was modeled by using the mass decay model, which facilitates the modeling with the weight disparity between ions and neutrals.[13] The mean velocity of electrons is given by the drift-diffusion model.[16]

$$\boldsymbol{u}_e = -[\mu_e]\boldsymbol{E} - \frac{[\mu_e]}{e}\frac{\nabla p_e}{n_e}, \quad \boldsymbol{E} = -\nabla\phi \tag{1}$$

$$[\mu_e] = \begin{pmatrix} \cos\theta & -\sin\theta \\ \sin\theta & \cos\theta \end{pmatrix}^{-1} \begin{pmatrix} \mu_{e,\perp} & 0 \\ 0 & \mu_{e,//} \end{pmatrix} \begin{pmatrix} \cos\theta & -\sin\theta \\ \sin\theta & \cos\theta \end{pmatrix} \tag{2}$$

Here θ is an angle of the magnetic field line relative to the axial axis. The elliptic equation with regard to the electric potential can be derived with Eq. (1) and the current conservation law.

$$\nabla \cdot n_e \left(\boldsymbol{u}_i - [\mu_e]\nabla\phi + \frac{[\mu_e]}{e}\frac{\nabla p_e}{n_e} \right) = 0 \tag{3}$$

The electron mobility perpendicular to the magnetic field includes the effect of Bohm-like diffusion, and then is defined as

$$\mu_{e,\perp} = \frac{1}{1+\beta_e^2}\frac{e}{m_e(\nu_{en}+\nu_{ei}+\nu_{Bohm})} \tag{4}$$

where

$$\beta_e = \frac{eB}{m_e(\nu_{en}+\nu_{ei}+\nu_{Bohm})}, \qquad \nu_{Bohm} = \frac{\alpha_B}{16}\omega_{c,e}\ . \tag{5}$$

The parameter α_B prescribes the degree of the Bohm diffusion, and was independently defined in several segmented domains in this simulation.[14] The electron transport along the magnetic field is generally considered to be much greater than the diffusion across the magnetic field. This anisotropic diffusion makes it difficult to solve Eq. (3) in an orthogonal mesh, and hence the electron equation is usually solved in the field-aligned-mesh.[17] In the preceding hybrid-PIC modeling,[12-15,18] the electron momentum equation along lines of force is approximated by the Boltzmann relation, and electron energy conservation perpendicular to the magnetic field is determined by means of quasi-one-dimensional approach. A fully-two-dimensional approach has also been developed in Hall2De,[6] i.e. no assumption was made regarding the rate of electron transport in the parallel and perpendicular directions of the magnetic field. Both approaches use field-aligned-mesh for solving the electron transport to avoid numerical difficulty caused by the anisotropic diffusion. It is known that the field-aligned-mesh provides more accurate solution than the regular mesh, but it requires high mesh quality near the boundary to obtain its inherent benefit.[19] In this study, we employed a simpler modeling for the electron transport along the magnetic field to facilitate the solution of Eq. (3) in a regular mesh.

When electrons move fast along the magnetic field, it is speculated that their velocity should be damped by some sort of instabilities such as electron-ion two-stream instability. Based on this assumption, the anomalous collision frequency regarding electron-ion two-stream instability was additionally involved in the definition of the electron mobility along the magnetic field in the whole computational region.

$$\mu_{e,//} = \frac{e}{m_e\left(\nu_{en} + \nu_{ei} + \nu_{anm}\right)} \tag{6}$$

where

$$\nu_{anm} = \left(\frac{m_e}{m_i}\right)^{1.3} f(M_e)\sqrt{2}\omega_{pe},\ \ f(M_e) = aM_e^b\ \ (M_e < 1.3),\quad f(M_e) = 1\ \ (M_e \geq 1.3),\quad M_e = \frac{\left|\boldsymbol{u}_{e,//}\right|}{\sqrt{kT_e/m_e}} \tag{7}$$

Here ω_{pe} is the electron plasma frequency. This anomalous collision frequency regarding the two-stream instability was originally introduced in the hollow cathode simulation by Mikellides to explain the anomalous resistivity in the plume region of hollow cathodes.[20] A modification was made in the definition of the drift Mach number M_e so that only the electron-velocity component parallel to the magnetic field is considered as a drift velocity. It should be noted that, with this modification, this anomalous term takes effect only when electron velocity has a component parallel to the magnetic field. In other words, this anomalous effect is vanished when electrons move exactly perpendicular to the magnetic field. It is expected that this model prevents excessive electron transport along the magnetic field, and consequently the anisotropic diffusion is alleviated, which will enable us to solve Eq. (3) directly in a regular mesh without difficulties regarding numerical instability. In addition, compatibility of this model with the simulation including the internally mounted cathode is quite well, because the electrons from the cathode are emitted nearly along the magnetic field. Since the anomalous resistivity regarding the two-stream instability or ion acoustic turbulence (IAT) is believed to be excited in the cathode plume region, the anomalous resistivity imposed along the magnetic field works naturally for the electrons emitted from the cathode.

The electron temperature was determined by solving the steady energy conservation equation which considers the electron kinetic energy.[9,21,22]

$$\nabla\cdot\left(\left(\frac{1}{2}\rho_e\boldsymbol{u}_e^2 + \frac{5}{2}n_e kT_e\right)\boldsymbol{u}_e - \frac{5n_e k^2 T_e}{2e}\left[\mu_e\right]\nabla T_e\right) = \boldsymbol{j}_e\cdot\boldsymbol{E} - Q_{ion} - Q_{exc} \tag{8}$$

Here Q_{ion} and Q_{exc} represent energy consumption due to ionization and excitation, respectively.[23] In the evaluation of the ionization rate, the electron kinetic energy as well as the thermal energy was taken into account.

Both Eqs. (3), (8) were discretized by Gelerkin finite element method, and were solved by a direct solver.[24] The PIC procedures were parallelized by means of a dynamic domain decomposition to make the load balance uniform.

C. Boundary Conditions

When Eq. (3) was solved, the thin sheath model was assumed on the anode boundary. The electron current density on the anode is given by,

$$j_{e,anode} = \frac{1}{4}en_e\sqrt{\frac{8kT_e}{em_e}}\exp\left(-\frac{e\left(\phi_p - \phi_a\right)}{kT_e}\right) \tag{9}$$

where ϕ_a and ϕ_p are the anode potential and the plasma potential, respectively. The above equation implicitly assumes an ion sheath ($\phi_p > \phi_a$), but the situation of $\phi_p < \phi_a$ was rarely occurred in the calculation condition shown later. On the cathode boundary, which corresponds to the keeper exit in this simulation, the space potential $\phi_c$was specified. On the other dielectric wall boundaries, the net current was set to zero. As mentioned earlier, the keeper wall was treated as a dielectric boundary condition for simplicity. To make the current path closed in the computational domain, the net current on the plume boundaries was also set to zero.

The electron thermal flux required to solve Eq. (8) is given by,

$$\text{Anode:}\ \ q_{e,anode} = \frac{1}{4}n_e\sqrt{\frac{8kT_e}{\pi m_e}}\exp\left(-\frac{e\left(\phi_p - \phi_a\right)}{kT_e}\right)\left(2kT_e + e\left(\phi_p - \phi_a\right)\right) \tag{10}$$

$$\text{Dielectric wall:}\ \ q_{e,BN} = \frac{\Gamma_i}{1-\gamma}\left(2kT_e + e\phi_{sh}\right) - \frac{\gamma\Gamma_i}{1-\gamma}\left(2kT_w + e\phi_{sh}\right) \tag{11}$$

where Γ_i, γ, ϕ_{sh} are the ion number flux, secondary electron emission coefficient, and sheath potential, respectively. The γ is given as a function of electron temperature,[23] and then the effect of space-charge limit was considered based on the Hobbs and Wesson theory.[25] The electron temperatures on the cathode boundary and the plume boundary were assumed to be constant values.

Since the wall boundaries correspond sheath edge due to the thin sheath assumption, the ions were assumed to inflow into the wall boundaries with the Bohm velocity. Therefore the ion density on the walls, determined from PIC, was corrected with the ion flux maintained.[26]

D. Calculation Condition

The calculation condition is summarized in Table 1. The mass flow rate from the anode was set to 5.0 mg/s, and the anode-to-cathode flow ratio was set to 12:1, because there are informative experimental data of SPT-100 measured under the same flow ratio for the widely-ranged back pressure.[27] In the experiment by Diamant et al, the mass flow rate was adjusted so that the discharge current was kept constant at 4.5 A for the varied back pressure. Since the anode mass flow rate of 5.0 mg/s corresponds to a back pressure of 3×10^{-5} Torr, we set the same back pressure in all simulations here. The cathode voltage, which means a space potential set at the keeper exit in this manuscript, is roughly considered to be between 10 – 20 V when viewed from a cathode body, thus we assumed it to be 10 V.

In the present model, the model parameters of α_B in Eq. (5) and a, b in Eq. (7) should be set. In this study, the computational domain was artificially decomposed into four regions as shown in Fig. 2, where each region is named as R1, R2, R3, and R4. The α_B in each region was independently determined so that the performance approached the experimental data of the actual SPT-100,[27] but the parameters a and b were set uniformly in the whole domain for simplicity. Table 2 shows the parameter sets examined in this study. The case1 is regarded as a benchmark case, and in case2, the lower α_B was used in R4 to see the effect of Bohm diffusion on the cathode plume.

Figure 3 shows the computational mesh used here. The mesh size within the acceleration channel is about 0.3 mm which is nearly the same order of magnitude as an estimated mean free path of the Coulomb collision between ions.

Table 1. Calculation Condition.

Working gas	Xenon
Anode mass flow rate	5.0 mg/s
Cathode mass flow rate	0.42 mg/s
Anode Voltage	300 V
Cathode Voltage (set at keeper exit)	10 V
Back pressure	3×10^{-5} Torr
Gas temp. of anode propellant	800 K
Gas temp. of cathode propellant	2000 K
Mach number of propellant at anode/cathode port	1.0
Ionization degree of cathode propellant	0.1
Electron temp. at plume boundary	3 eV
Electron temp. at cathode boundary	1.5 eV

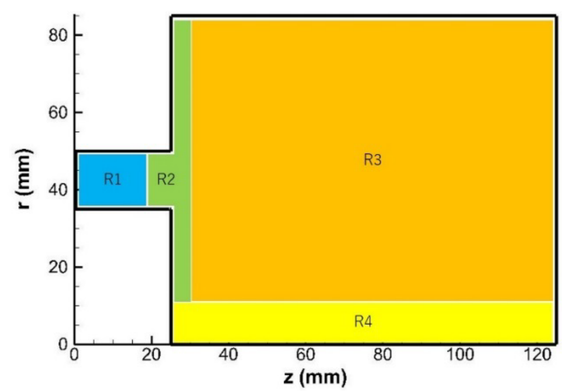

Figure 2. Domain decomposition used for setting model parameters.

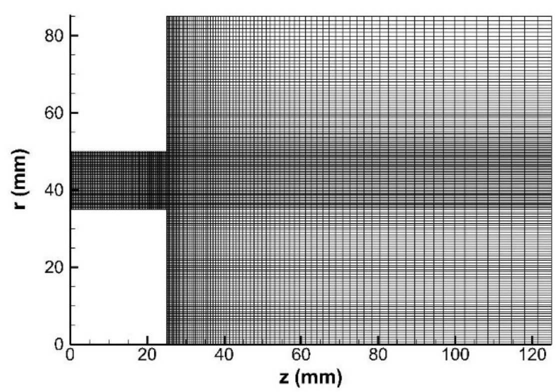

Figure 3. Computational mesh.

Table 2. Model parameters.

	Region	α_B	a	b
Case1	R1	0.085	0.3	0.25
	R2	0.15	0.3	0.25
	R3	10	0.3	0.25
	R4	10	0.3	0.25
Case2	R1	0.085	0.3	0.25
	R2	0.15	0.3	0.25
	R3	10	0.3	0.25
	R4	0.5	0.3	0.25

III. Results and Discussion

A. Plasma Characteristics

The electron density, electric potential, and electron temperature distributions in case1 and case2 are shown in Figs. 3 and 4, respectively. In both cases, the electron density has a peak about 1.6×10^{18} m^{-3} in the acceleration channel, which is consistent with the preceding result of HPHALL-2.[18] The electron density seems to be slightly shrunk near the channel exit. This might be associated with the radial potential distribution around the density's peak, where the potential has concaved radial profile in the downstream direction. As the preceding results,[18] however, the rapid decrease in the electric potential near the thruster exit can be seen, and also the isothermal characteristic of the electron temperature still holds along the magnetic field in spite of the introduced anomalous resistivity along the magnetic field. One of the concerns will be the extent of deviation from the Boltzmann relation along the magnetic field. This can be evaluated by confirming if a thermalized potential ϕ_{th} is constant along the magnetic field.

$$\phi_{th} = \phi - T_e \ln(n_e). \tag{12}$$

The contour lines of the thermalized potential are compared with the magnetic lines of force in Fig. 5. The result demonstrates that the contour line of the thermalized potential is almost overlapped with the lines of force. Considering these facts, it can be said that the proposed model can provide results consistent with the preceding numerical studies using the field-aligned mesh. This suggests that the additional anomalous resistivity along the magnetic field hardly hinders the capability of capturing the essence of physics, and mainly plays a role in stabilizing the numerical procedures.

In the cathode plume region, the peak of the electron density is found at the cathode exit about 2×10^{19} m^{-3} for case1 and 5×10^{19} m^{-3} for case2. According to the results of the probe measurement of a hollow cathode,[28] the order of magnitude of electron density in the vicinity of the keeper exit is 10^{19} m^{-3} for the condition of 0.54 mg/s, 25 A cathode. Therefore, the present result for a cathode flow rate of 0.42 mg/s seems to be reasonable, whereas the discharge current is much lower than the experimental condition as shown later. The reason for the higher electron density of case2 is the potential well appeared in front of the cathode, where the ions are supposed to be gathered from the surroundings, and the ions ejected from the cathode hardly overcome the potential barrier. In case2, the potential well is grown due to the lower Bohm diffusion in this region. Since the lower effective collision frequency decreases the electron mobility perpendicular to the magnetic field, resistivity is supposed to increase in the radial direction, which results in growth of the potential well. Such a potential well in front of the cathode has been observed in preceding experimental studies,[29] hence the result of case2 is qualitatively preferable to that of case1. The reason for the lower Bohm diffusion around the cathode might be an open question, but if the fluctuating electric field induced by IAT is directed almost axially around the cathode, E×B drift caused by the fluctuating field hardly grow because of the axially aligned magnetic field in this region, which might be one of possible reasons for the lower Bohm diffusion in front of the cathode.

B. Thrust performance

The thrust performances for both cases are shown in Table 3. The experimental values were estimated from the fitting formula shown in Ref. 27 at a back pressure of 3×10^{-5} Torr. As mentioned earlier, the model parameters for case1 shown in Table 2 are determined so that the simulated performance approached the experimental values. The results indicate that the performance is insensitive to the coefficient of Bohm diffusion in the cathode region, which is consistent with the preceding numerical study.[29]

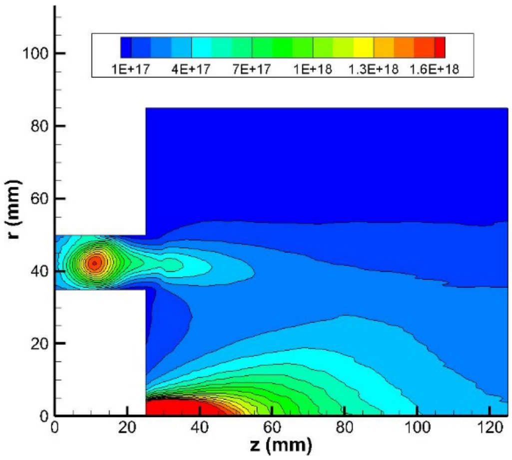

(a) Electron number density, m^{-3}.

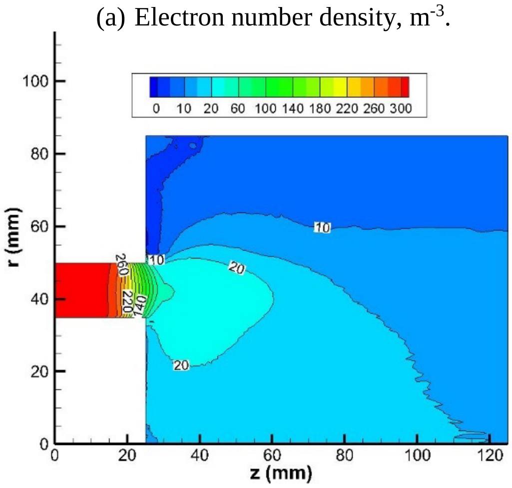

(b) Electric potential, V.

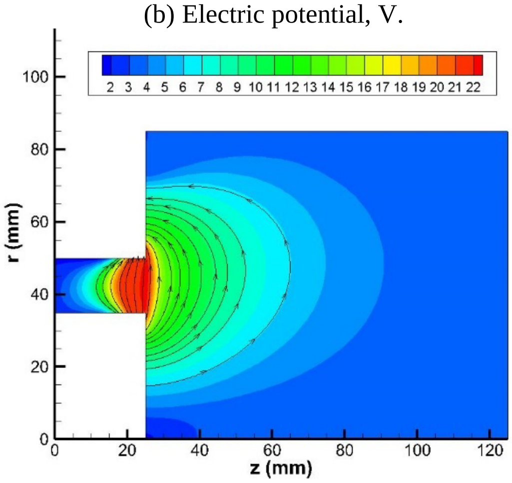

(c) Electron temperature, eV.

Figure 4. Plasma characteristics in case1. *In (b) electric potential, the interval of the contour lines blow 20 V is 5 V. In (c) electron temperature, the magnetic field lines are overlapped.*

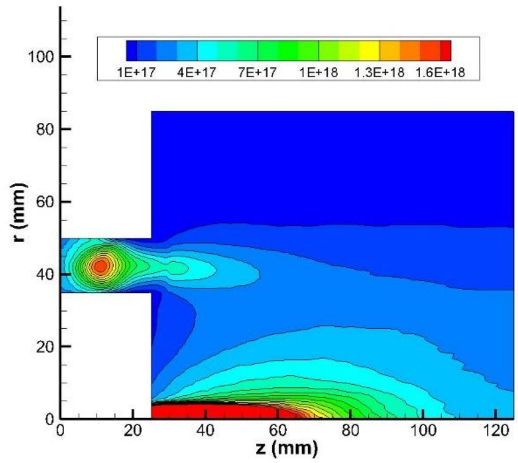

(a) Electron number density, m^{-3}.

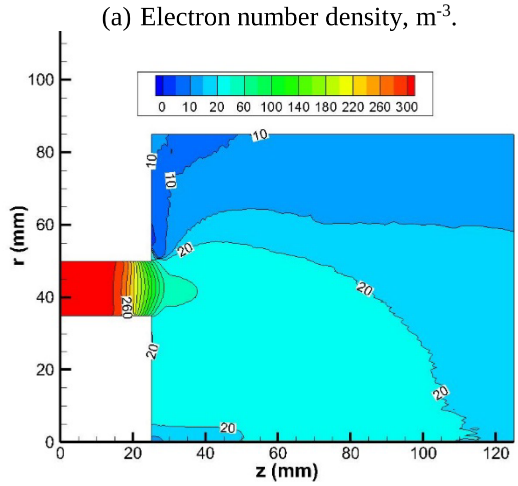

(b) Electric potential, V.

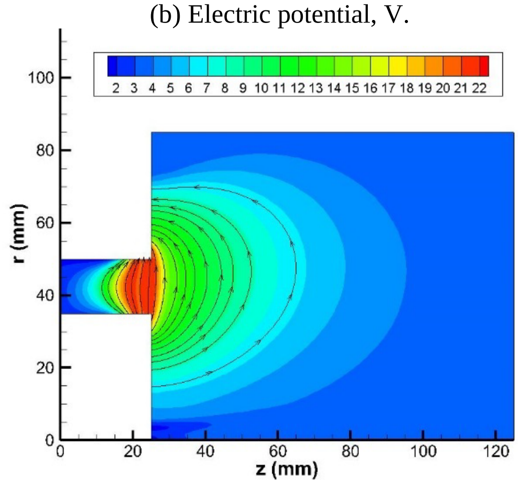

(c) Electron temperature, eV.

Figure 5. Plasma characteristics in case2. *In (b) electric potential, the interval of the contour lines blow 20 V is 5 V. In (c) electron temperature, the magnetic field lines are overlapped.*

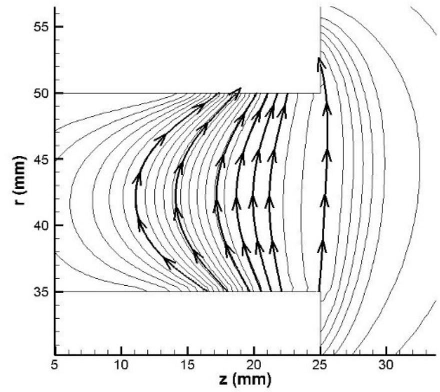

Figure 6. Comparison between thermalized potential and the magnetic lines of force for case1. *The lines with arrows is the magnetic lines of force.*

Table 3. Thrust Performances. *The experimental data were measured for the conventional SPT-100 thruster with an external cathode.[27] The experimental values are calculated with fitting formulas at a back pressure of 3×10^{-5} Torr. Note that the model parameters for case1 were determined so that the simulated performance approached the experimental values.*

	Thrust (mN)	Discharge Current (A)	Thrust Efficiency
Case1	82.7	4.57	45.8
Case2	82.4	4.51	46.0
Exp.	82.7	4.50	46.4

IV. Conclusion

The plasma flow of a Hall thruster with an internally mounted cathode was simulated by using hybrid-PIC model. In the model of electron mobility, the anomalous resistivity along the magnetic field is introduced to avoid excessive electron transport along the magnetic field, and to stabilize the numerical procedures in a regular mesh. To confirm the feasibility of the suggested model and to discuss qualitative properties of the Hall thruster with an internally mounted cathode, SPT-100 with an imaginary internal cathode was selected as a simulation target.

The results show that the peak of electron density is quantitatively consistent with the preceding studies, and the anomalous resistivity along the magnetic field hardly interfere with capturing basic properties such as isothermal characteristics of electron temperature along the magnetic field. It was also shown that the potential well can be formed by reducing the extent of Bohm diffusion in front of the cathode, and the performance of the thruster is insensitive to the extent of Bohm diffusion around the cathode.

References

[1]Duchemin, O., Méhauté, D. L., Öberg, M., Cavelan, X., Guilhem-Ducléon, M., Khimeche, G., Payot, F., Soubrier, L., Galiana, D., and Glorieux, G., "End-to-End Testing of the PPS®5000 Hall Thruster System With a 5-kW Power Processing Unit," IEPC-2015-127, 2015.

[2]Hofer, R., Kamhawi, H., Herman, D., Polk, J., Snyder, J. S., Mikellides, I., Huang, W., Myers, J., Yim, J., Williams, G., Ortega, A. L., Jorns, B., Sekerak, M., Griffiths, C., Shastry, R., Haag, T., Verhey, T., Gilliam, B., Katz, I., Goebel, D., Anderson, J. R., Gilland, J., and Clayman, L., "Development Approach and Status of the 12.5 kW HERMeS Hall Thruster for the Solar Electric Propulsion Technology Demonstration Mission," IEPC-2015-186, 2015.

[3]Welander, B., Monheiser, J., Meckel, N., Grys, K. d., and Peterson, P., "Demonstration of the XR-12 Hall Current Thruster," IEPC-2013-451, 2013.

[4]Funaki, I., Iihara, S., Cho, S., Kubota, K., Watanabe, H., Fuchigami, K., and Tashiro, Y., "Laboratory Testing of Hall Thrusters for All-electric Propulsion Satellite and Deep Space Explorers," AIAA-2016-4942, 2016.

[5]Goebel, D. M., Jameson, K. K., and Hofer, R. R., "Hall Thruster Cathode Flow Impact on Coupling Voltage and Cathode Life," *Journal of Propulsion and Power*, Vol. 28, No. 2, 2012, pp. 355-363.

[6]Mikellides, I. G., Ortega, A. L., Katz, I., and Jorns, B. A., "Hall2De Simulations with a First-principles Electron Transport Model Based on the Electron Cyclotron Drift Instability," AIAA-2016-4618, 2016.

[7]Choi, M., and Boyd, I. D., "Numerical Simulation of Keeper Erosion in a 6-kW Laboratory Hall Thruster," IEPC-2015-16, 2015.

[8]Cho, S., Kubota, K., Watanabe, H., Hara, K., and Funaki, I., "Comparing Internal and External Cathode Boundary Position in a Hall Thruster Particle Simulation," IEPC-2017-402, 2017.

[9]Kubota, K., Oshio, Y., Watanabe, H., Cho, S., Ohkawa, Y., and Funaki, I., "Numerical and Experimental Study on Discharge Characteristics of High-Current Hollow Cathode," AIAA-2016-4628, 2016.

[10]Kubota, K., Oshio, Y., Watanabe, H., Cho, S., Ohkawa, Y., and Funaki, I., "Hybrid-PIC Simulation on Plasma Flow of Hollow Cathode," *Trans. JSASS Aerospace Tech. Japan,* Vol. 14, No. ists30, 2016, pp. Pb_189-Pb_195.

[11]Kubota, K., Cho, S., Watanabe, H., and Funaki, I., "Hall Thruster Simulation by Hybrid-PIC with Magnetic Field-Aligned Resistivity," Proceedings of 59th Space Sciences and Technology Conference, JSASS-2015-4046, 2015. (in Japanese)

[12]Fife, J. M., and Martinez-Sanchez, M., "Two-dimensional Hybrid Particle-In-Cell(PIC) Modeling of Hall Thrusters," IEPC-1995-240, 1995.

[13]Parra, F. I., Ahedo, E., Fife, J. M., and Martínez-Sánchez, M., "A two-dimensional hybrid model of the Hall thruster discharge," *Journal of Applied Physics,* Vol. 100, No. 2, 2006, p. 023304.

[14]Hofer, R. R., Katz, I., Mikellides, I. G., Sullivan, R. M., Goebel, D. M., Jameson, K. K., Sullivan, R. M., and Johnson, L. K., "Efficacy of Electron Mobility Models in Hybrid-PIC Hall Thruster Simulations," AIAA-2008-4924, 2008.

[15]Koo, J. W., and Boyd, a. I. D., "COMPUTATIONAL MODEL OF AN SPT-100 THRUSTER," IEPC-2003-0071, 2003.

[16]Komurasaki, K., and Arakawa, Y., "Two-Dimensional Numerical Model of Plasma Flow in a Hall Thruster," *Journal of Propulsion and Power,* Vol. 11, No. 6, 1995, pp. 1317-1323.

[17]Pérez-Grande, D., Fajardo, P., and Ahedo, E., "Benchmarks for Magnetic Field Aligned Meshes in Electromagnetic Plasma Thruster Simulations," IEPC-2015-203, 2015.

[18]Hofer, R. R., "Wall Sheath and Electron Mobility Modeling in Hybrid-PIC Hall Thruster Simulations," Vol. AIAA 2007-5267, 2007.

[19]Samuel J. Araki, a. R. E. W., "Automatic Magnetic Field Aligned Mesh Generation for a Ring-Cusp Discharge Chamber," AIAA-2014-3830, 2014.

[20]Mikellides, I. G., Katz, I., Goebel, D. M., and Jameson, K. K., "Evidence of nonclassical plasma transport in hollow cathodes for electric propulsion," *Journal of Applied Physics,* Vol. 101, No. 6, 2007, p. 063301.

[21]Hara, K., and Boyd, I. D., "Low Frequency Oscillation Analysis of a Hall Thruster Using a One-Dimensional Hybrid-Direct Kinetic Simulation," IEPC-2013-266, 2013.

[22]Hagelaar, G. J. M., Makasheva, K., Garrigues, L., and Boeuf, J. P., "Modelling of a dipolar microwave plasma sustained by electron cyclotron resonance," *Journal of Physics D: Applied Physics,* Vol. 42, No. 19, 2009, p. 194019.

[23]Goebel, D. M., and Katz, I., *Fundamentals of Electric Propulsion: Ion and Hall Thrusters*: JOHN WILEY & SONS, INC., 2008.

[24]Amestoy, P. R., Duff, I. S., L'Excellent, J.-Y., and Koster, J., "A fully asynchronous multifrontal solver using istributed dynamic scheduling," *SIAM Journal of Matrix Analysis and Applications,* Vol. 23, No. 1, 2001, pp. 15-41.

[25]Hobbs, G. D., and Wesson, J. A., "Heat flow through a Langmuir sheath in the presence of electron emission," *Plasma Physics,* Vol. 9, No. 1, 1967, pp. 85-87.

[26]Parra, F. I., and Ahedo, E., "Fulfillment of the Bohm Condition on the 'HPHALL' Fluid-PIC Code," AIAA-2004-3955, 2004.

[27]Diamant, K. D., Liang, R., and Corey, R. L., "The Effect of Background Pressure on SPT-100 Hall Thruster Performance," AIAA 2014-3710, 2014.

[28]Goebel, D. M., Jameson, K. K., Watkins, R. M., Katz, I., and Mikellides, I. G., "Hollow cathode theory and experiment. I. Plasma characterization using fast miniature scanning probes," *Journal of Applied Physics,* Vol. 98, No. 11, 2005, p. 113302.

[29]Ortega, A. L., and Mikellides, I. G., "The importance of the cathode plume and its interactions with the ion beam in numerical simulations of Hall thrusters," IEPC-2015-310, 2015.